

# The Effect of Overlap between Absorption Coefficients on the Variation of Current Densities in Intermediate Band Solar Cells

Navruz T. S.

Gazi University, Faculty of Engineering and Architecture, Department of Electrical and Electronics Engineering,  
Maltepe, Ankara, Turkey  
[selcen@gazi.edu.tr](mailto:selcen@gazi.edu.tr)

## Abstract

Intermediate band solar cell (IBSC) has a structure that absorbs the subbandgap photons by the help of the intermediate band (IB) located inside its base region and increases the photocurrent without decreasing the output voltage. In this study, detailed balance equations are used to investigate the current density (total, electron and hole currents) variations of IBSC with IB energy level, under nonoverlap and overlap conditions, in the cases of equal and nonequal absorption coefficients, for  $E_G=1.95$  eV. It is obtained that in both cases; the IBSC has two optimum IB levels, one below half of the band gap and the other above half of the bandgap, under nonoverlap condition. The optimum IB levels shift towards the half of the bandgap under overlap condition in the case of equal absorption coefficients. If the new optimum IB levels are used, the current contribution of IB level becomes independent of overlap. But the current resulting from the transitions between valance band to conduction band decreases sharply from  $26 \text{ mA/cm}^2$  to  $8 \text{ mA/cm}^2$ . when overlap increases from 0 to 4 eV. The reduction in this current is compensated in the case of nonequal absorption coefficients.

## 1. Introduction

The most important factor that restricts the efficiency of conventional p-n junction solar cells is the nonabsorption of the photons with energies lower than the semiconductor bandgap. IBSC has a structure capable of absorbing the below bandgap photons by the help of a half-filled intermediate band situated inside its bandgap, [1], as seen in Fig. 1. The detailed explanation of the operational principles of IBSC can be found in [2-3]. The theoretical efficiency limit of IBSC with one IB is 63.2%, under fully concentrated sun light (46000 sun) from a thermal source at 6000 K, when the cell is at 300 K for  $E_G=1.95$  eV [1-3]. When impact ionization is effective, the high energy photons can also be used to produce multi-carrier generation [3,4-5]. The efficiency is obtained as 85% when the number of IB level is infinite. [6]. Theoretical studies are carried out on IBSCs using detailed balance equations [1-3,7] and quasi-drift diffusion model [8]. The experimental results on the

implementation of IBSC are reported in [9] but no improvement in efficiency is obtained yet.

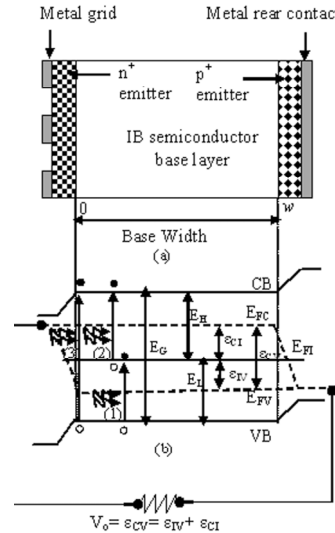


Fig.1 (a) General structure of IBSC, (b) Energy band diagram and photon absorption processes involved in IBSC

IBSC has three absorption coefficients,  $\alpha_{CV}$ ,  $\alpha_{IC}$ , and  $\alpha_{VI}$ , representing the probability of a photon being absorbed through three of the generation processes; (1) from valance band (VB) to IB, (2) from IB to conduction band (CB) and (3) from VB to CB. If only one of the three absorption coefficients is valid in a particular energy interval, it is called as nonoverlap condition. If two or more absorption coefficients are valid, then it is called overlap condition (See Fig. 2). The shape and the value of absorption coefficients corresponding to different transitions depend on the occupation of electronic states. But absorption coefficients are assumed to be constant in the energy intervals shown in Fig. 2a and b, for simplicity, in the calculations [2-3]. The equal absorption coefficients ( $\gamma=1$  case) illustrated in Fig. 2.a and the nonequal absorption coefficients ( $\gamma=10$  case) given in Fig. 2.b are used in this study.

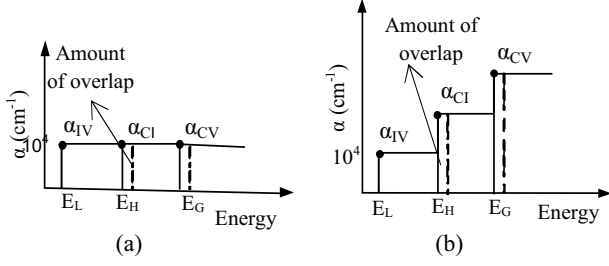


Fig.2 The variation of absorption coefficients due to the energy in the cases of equal (a) and nonequal (b) absorption coefficients

The influences of overlap on the efficiency of IBSC and the position of the optimum IB level were investigated in detail in our previous studies, especially for  $E_G=1.95$  eV and 1.12 eV [2-3]. In this study, the variation of IBSC current density due to the IB energy level, under nonoverlap and overlap conditions will be analyzed in the cases of  $\gamma=1$  and 10, for  $E_G=1.95$  eV, for the first time. The variation of optimum IB level position with the amount of overlap will be explained more clearly by obtaining the electron and hole current densities through the IB.

## 2. Mathematical Model

Detailed balance method is used in this study to obtain the current-voltage characteristics of IBSC. The current density equations due to the generation and recombination of electrons and holes, ignoring the emitter contributions, SRH recombination and the Auger effect, are given as below:

$$J_{gen} = e \int_0^w [G_{CV} + G_{IC/VI}] dx \quad (1.a)$$

$$J_{rec,1} = e \int_0^w [R_{CV}^{Rad} + R_{CI}^{Rad} + R_{CV,CI}^{int} + R_{CI,IV}^{int}] dx \quad (1.b)$$

$$J_{rec,2} = e \int_0^w [R_{CV}^{Rad} + R_{IV}^{Rad} + R_{CV,IV}^{int} + R_{IV,CI}^{int}] dx \quad (1.c)$$

where  $w$  is the base width and  $e$  is the electron charge. In Eq. 1.a,  $J_{gen}$  represents the generation current density that constitutes the short circuit current density of the IBSC.  $J_{rec,1}$  and  $J_{rec,2}$  correspond to the recombination current densities of electrons and holes, respectively. The generation and the recombination rate terms will be clarified in the following paragraphs.

The photo-generation rate due to the electron transitions from VB to CB,  $G_{CV}(x)$ , is expressed as below:

$$G_{CV}(x) = \int_{\epsilon} \alpha_{CV} F_0 \exp(-\alpha_{TOT} x) d\epsilon \quad (2)$$

where  $\epsilon$  is the energy,  $\alpha_{TOT} = \alpha_{CV} + \alpha_{CI} + \alpha_{IV}$  and  $F_0$  corresponds to the number of photons, in the energy interval of  $\epsilon$  and  $\epsilon+d\epsilon$ , per second hitting per unit area of the front surface of the cell.  $F_0$  is given by [8]:

$$F_0 = X \frac{2\pi}{h^3 c^2} \sin^2 \theta_S \frac{\epsilon^2}{\exp\left(\frac{\epsilon}{k_B T_S}\right) - 1} \quad (3)$$

where,  $X$  represents the sun concentration that is chosen as 46000 in this study.  $c$  is speed of light,  $h$  is Planck constant and  $\theta_S$  is the semi-angle of the sun solar disk sustained from the Earth ( $\sin^2 \theta_S = 1/46000$ ).  $k_B$  denotes the Boltzmann constant and  $T_S$  is the sun temperature. The photo-generation rates due to the

transitions from VB to IB and from IB to CB are obtained in a similar way. The current density due to  $G_{CV}(x)$  is:

$$J_{CV} = e \int_0^w [G_{CV}] dx \quad (4)$$

$G_{CV}(x)$  occurs in both single gap solar cells and the IBSCs. The current improvement is provided by  $G_{VI}(x)$  and  $G_{IC}(x)$ . The current densities generated through the IB are expressed as below.

$$J_{genB,1} = e \int_0^w [G_{IC}(x)] dx \quad (5.a)$$

$$J_{genB,2} = e \int_0^w [G_{VI}(x)] dx \quad (5.b)$$

$J_{genB,1}$  and  $J_{genB,2}$  are the current densities resulting from the emptying and filling processes of IB, respectively. The current density provided through the IB is limited by the smaller one of the generated currents. The optimum IB energy level of an IBSC is obtained when both currents become equal.

$R_{CV}^{Rad}$ , is the radiative recombination rate due to the electron transitions from CB to VB.

$$R_{CV}^{rad} = \frac{2\pi}{h^3 c^2} \int_{\epsilon} \left[ \alpha_{CV} \left( \frac{A}{\alpha_{TOT}} \right) \exp(-\alpha_{TOT} w) \epsilon^2 \right] d\epsilon \quad (6)$$

where,

$$A = \alpha_{CV} v_{CV} + \alpha_{CI} v_{IC} + \alpha_{IV} v_{VI} \quad (7)$$

Here  $v_{IC}$ ,  $v_{VI}$  and  $v_{CV}$  are the Bose-Einstein factors related with the amount of quasi Fermi level splitting [7].  $R_{CI}^{Rad}$  and  $R_{IV}^{Rad}$  are evaluated in a similar way.

$R_{CV/VI}^{int}$ ,  $R_{IC/IC}^{int}$ ,  $R_{IC/VI}^{int}$  and  $R_{VI/IC}^{int}$  are the internal recombination rate terms due to the overlap between absorption coefficients  $\alpha_{CV}-\alpha_{VI}$ ,  $\alpha_{CV}-\alpha_{CI}$  and  $\alpha_{IC}-\alpha_{VI}$ , respectively.

$$R_{CV/VI}^{int} = \frac{8\pi^2}{h^3 c^2} \int_{\epsilon} \left( \frac{\alpha_{CV} \alpha_{VI}}{\alpha_{TOT}} (v_{CV} - v_{VI}) \right) \epsilon^2 d\epsilon \quad (8)$$

As seen from Eq.7, internal recombination terms are zero when there is no overlap between absorption coefficients.

$R_{CV/IC}^{int}$ ,  $R_{IC/VI}^{int}$  and  $R_{VI/IC}^{int}$  can be found similarly.

$J_{rec,1}$  and  $J_{rec,2}$  terms in Eq. (1.b and c) are equalized to obtain the  $J$ - $V$  characteristics of an IBSC. The output voltage  $V_o$  equals to the summation of the quasi-Fermi level splits.

$$eV_o = \epsilon_{IV} + \epsilon_{CI} = \epsilon_{CV} \quad (9)$$

So, an equation including two unknowns,  $\epsilon_{IV}$  and  $\epsilon_{CI}$ , is obtained. By using  $\epsilon_{CI} = eV_o - \epsilon_{IV}$  and solving the equation for each value of  $eV_o$ , the variation of the current density,  $J = J_{gen} - J_{rec}$ , versus the output voltage is obtained.

Finally, the efficiency of IBSC is calculated as below:

$$\eta = \frac{P_m}{P_m} = \frac{J_m V_m}{P_m} = \frac{J_{sc} V_{oc} FF}{P_{in}} \quad (10)$$

Here,  $J_m$  and  $V_m$  are the current density and output voltage values at the maximum power point ( $P_m$ ).  $P_{in}$  is the incident

power density.  $J_{sc}$  corresponds to the short circuit current density,  $V_{oc}$  designates the open circuit voltage and  $FF$  represents the fill factor.

### 3. Numerical Results and Discussion

In this study, the variation of IBSC current density with the IB energy level is investigated under nonoverlap and overlap conditions, in the cases of equal and nonequal absorption coefficients, for  $E_G=1.95$  eV.  $E_G=1.95$  eV is preferred for analysis since it is the optimum bandgap providing the maximum efficiency for IBSCs [1-3]. During calculations, it is assumed that the carrier mobilities are infinite, no current is extracted from IB, all transitions between three bands are radiative and sun concentration is at maximum (46000). The following statement is used for equal ( $\gamma=1$ ) and nonequal ( $\gamma=10$ ) absorption coefficients.

$$\gamma = \alpha_{CVA} / \alpha_{ICA} = \alpha_{ICA} / \alpha_{VA} = \alpha_{VA} / \alpha_{CV} = \alpha_{CV} / \alpha_{IC} = \alpha_{IC} / \alpha_{VI} \quad (11)$$

The base layer thickness is determined from the product of the absorption coefficient and the base thickness ( $\alpha w$ ).  $\alpha w$  value is chosen as 5 for nonoverlap condition that requires  $\alpha w \geq 5$ , while the optimum value of  $\alpha w$  that was calculated in our previous study [2] is used for overlap condition. Optimum  $\alpha w$  values for each overlap conditions are given in Table 1.

Table 1 Optimum  $\alpha w$  values under 0, 0.4 and 4 eV overlap conditions and in the cases of  $\gamma=1$  and 10 [2].

Amount of overlap (eV)	$\gamma$	Optimum $\alpha w$
0	1	$\geq 5$
	10	$\geq 5$
0.4	1	2.7
	10	2
4	1	1.4
	10	2

In our previous study, the effect of overlap on the performance of IBSC was investigated in detail. It was found that the efficiency versus IB energy level curve was “M” shaped and had two peak points at nearly one third and two third of the bandgap, in both  $\gamma=1$  and 10 cases [2-3]. The peak points (optimum IB levels) shifted towards the half of the bandgap as the amount of overlap increased and became a single peak point at maximum overlap, in the case of  $\gamma=1$ . In addition to this a significant amount of reduction in the efficiency was observed. The reduction in the efficiency was compensated and the optimum IB level variation was negligible in the case of  $\gamma=10$  [2-3].

In this study, the variation of IBSC current density, at maximum power point, with IB energy level is obtained in the cases of  $\gamma=1$  and 10, under nonoverlap and overlap conditions to provide a clear explanation for the efficiency variation due to the IB energy level. The electron and hole short circuit current densities through IB ( $J_{genB,1}/X$  and  $J_{genIB}/X$ ) and the short circuit current density resulted from the electron transition from VB to CB ( $J_{CV}/X$ ) are also obtained to show how the optimum IB level is determined. The efficiency of IBSC depends on both the IBSC current density and output voltage. But this paper only

deals with IBSC current density since current density is much more effective on the variation of efficiency due to the overlap.

### 3.1. Variation of total current density

Fig. 3.a and b show the variation of total current density, at maximum power point, with the IB energy level under nonoverlap and overlap conditions, in the cases of  $\gamma=1$  and 10, respectively. The shapes of the curves are just like the efficiency-IB level curves that were found in our previous studies [2-3]. Under nonoverlap condition, the total current density has also two peak points at one third and two third of the bandgap in the cases of both  $\gamma=1$  and 10.

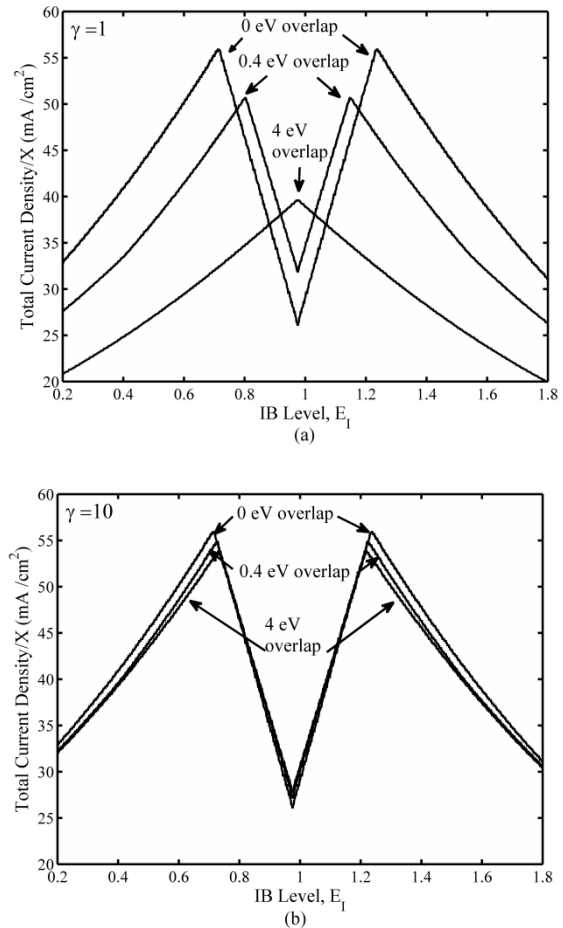


Fig. 3 Total current density/X versus IB level curves, for  $E_G=1.95$  eV in the cases of  $\gamma=1$  (a) and  $\gamma=10$  (b), under OV conditions of 0 eV , 0.4 eV and 4 eV

In  $\gamma=1$  case, the two peak points of the total current density decrease and shift towards the half of the bandgap with the amount of overlap. The single peak point is observed under maximum overlap (4 eV) condition. The peak points are obtained at the optimum IB levels found in the previous studies [2-3]. In the case of  $\gamma=10$ , the reduction in the peak points of total current density is compensated and optimum IB levels remained nearly constant. As a result, it can be said that the variation of efficiency in  $\gamma=1$  case should be larger than  $\gamma=10$  case.

### 3.2. Variations of $J_{CV}/X$ and electron/hole current densities through IB in the case of $\gamma=1$

The electron and hole current densities through IB and the current density resulting from the electron transition between VB to CB are obtained under nonoverlap condition, in the case of  $\gamma=1$ . As seen from Fig. 4,  $J_{CV}/X$  is independent of the position of IB level. The current enhancement in IBSCs is provided by the currents,  $J_{genIB,1}/X$  and  $J_{genIB,2}/X$ , resulting from the filling and emptying processes of IB. As seen from Fig.4, hole current density increases as the IB level becomes close to the VB and electron current density increases as the IB level becomes close to the CB. When an electron occupying a state in the IB is not transferred to the CB, it recombines and does not contribute to the photocurrent. Therefore, the efficiency improvement resulting from the intermediate band is limited by the smaller one of the electron and hole current densities through IB. Consequently, the optimum efficiency is obtained when these two currents become equal. In Fig.4,  $J_{genIB,1}/X$  and  $J_{genIB,2}/X$  are equal at  $E_I=0.71$  eV and 1.24 eV where the total current density and the efficiency are maximum [2-3].

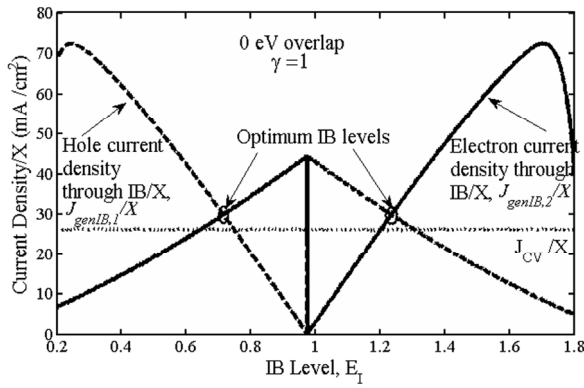


Fig.4. Electron (solid line) and hole (dashed line) current densities/ $X$  through IB and  $J_{CV}/X$  (dotted line) versus IB level curves, for  $E_G=1.95$  eV in the case of  $\gamma=1$ , under nonoverlap condition

As seen from Figures 5 and 6, the IB level where  $J_{genIB,1}/X$  and  $J_{genIB,2}/X$  are equal (optimum IB levels) shift towards the half of the bandgap as the amount of overlap increases, and become equal just at the half of the bandgap under maximum overlap condition. When the new optimum IB levels are used, the current contribution of IB is nearly independent of the overlap at 30 mA/cm<sup>2</sup>. However,  $J_{CV}/X$  decreases from 26 mA/cm<sup>2</sup> to 8.8 mA/cm<sup>2</sup>, when overlap increases from 0 to 4 eV. If there is no overlap, a photon with  $h\nu > E_G$ , is absorbed causing a transition between only VB to CB. But, if there is overlap, it can be absorbed causing a transition between the subbandgaps, VB to IB or IB to CB. Therefore the excess energy of the photon is wasted. As a result, the high energy photons are absorbed by subbandgaps and the photocurrent density is reduced under overlap condition. This effect is compensated by changing the position of the IB level for  $J_{genIB,1}/X$  and  $J_{genIB,2}/X$ . But the reduction in  $J_{CV}/X$  causes an important amount of reduction in the efficiency (nearly %20) [2-3].

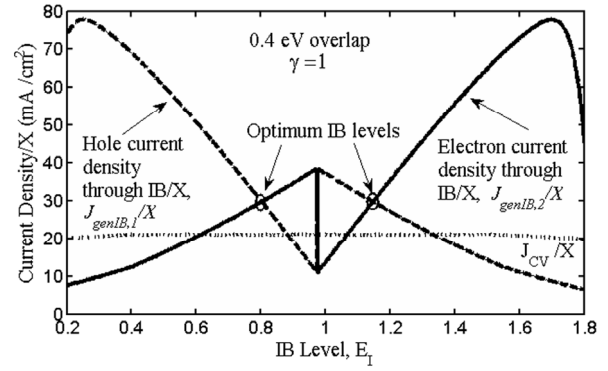


Fig.5. Electron (solid line) and hole (dashed line) current densities/ $X$  through IB and  $J_{CV}/X$  (dotted line) versus IB level curves, for  $E_G=1.95$  eV in the case of  $\gamma=1$ , under 0.4 eV overlap condition

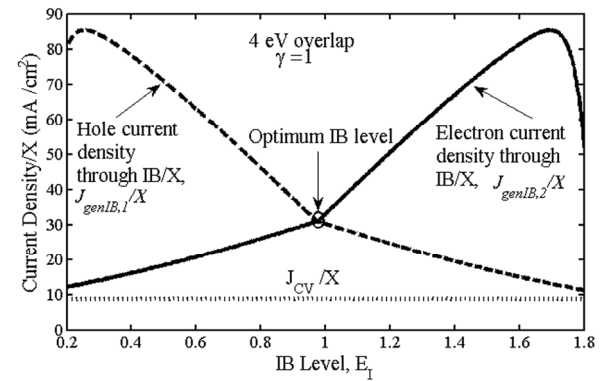


Fig.6. Electron (solid line) and hole (dashed line) current densities/ $X$  through IB and  $J_{CV}/X$  (dotted line) versus IB level curves, for  $E_G=1.95$  eV in the case of  $\gamma=1$ , under 4 eV overlap condition

### 3.3. Variations of $J_{CV}/X$ and electron/hole current densities through IB in the case of $\gamma=10$

As mentioned in our previous study, the effect of overlap is minimized, when the absorption coefficients increase with energy [2-3]. The variation of current densities  $J_{genIB,1}/X$ ,  $J_{genIB,2}/X$  and  $J_{CV}/X$  with the IB level are obtained in the case of  $\gamma=10$ , under 0-4 eV overlap conditions as seen in Figures 7-9.

When there is no overlap, the current density variations with IB level, in the case of  $\gamma=10$  is similar to the  $\gamma=1$  case (See Fig. 4 and 7). The current contribution of the IB level and the positions optimum IB levels (where  $J_{genIB,1}$  and  $J_{genIB,2}$  are equal) are independent of overlap. The reduction of  $J_{CV}/X$  with the amount of overlap is compensated in the case of  $\gamma=10$  with respect to  $\gamma=1$  case. So the efficiency decreases with an amount of only 6% in  $\gamma=10$  case [2-3].

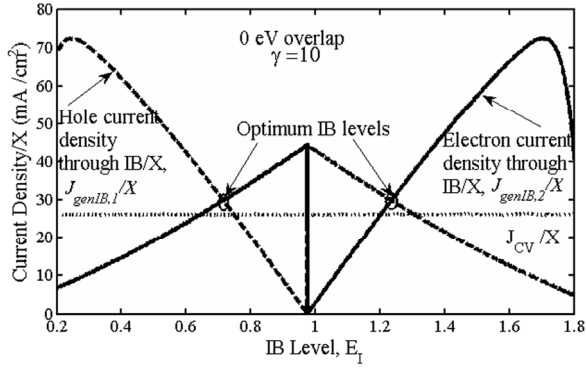


Fig.7. Electron (solid line) and hole (dashed line) current densities/X through IB and  $J_{CV}/X$  (dotted line) versus IB level curves, for  $E_G=1.95$  eV, in the case of  $\gamma=10$ , under 0 eV overlap condition

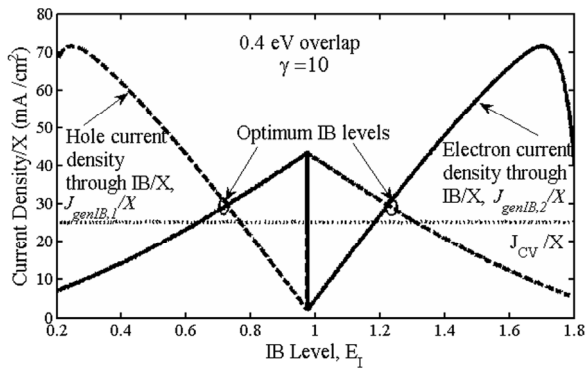


Fig.8. Electron (solid line) and hole (dashed line) current densities/X through IB and  $J_{CV}/X$  (dotted line) versus IB level curves, for  $E_G=1.95$  eV, in the case of  $\gamma=10$ , under 0.4 eV overlap condition

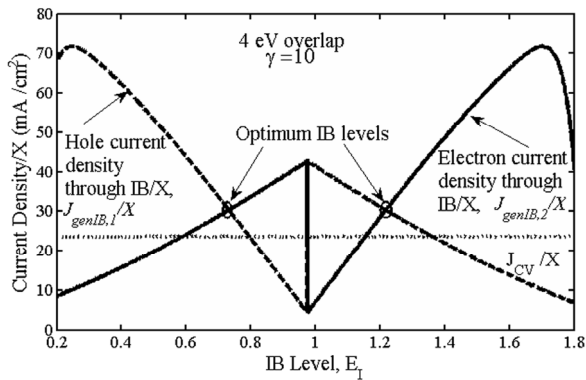


Fig.9. Electron (solid line) and hole (dashed line) current densities/X through IB and  $J_{CV}/X$  (dotted line) versus IB level curves, for  $E_G=1.95$  eV, in the case of  $\gamma=10$ , under 4 eV overlap condition

As a result,  $\gamma=10$  case seems to have advantage on  $\gamma=1$  case from the perspective of efficiency. But an important drawback of this case is the requirement of larger base width that is

determined by the reciprocal of the smallest absorption coefficient [2].

#### 4. Conclusions

In this study, the variation of IBSC current density with the IB energy level has been investigated using detailed balance equations, under nonoverlap and overlap conditions, in the cases of equal ( $\gamma=1$ ) and nonequal ( $\gamma=10$ ) absorption coefficients, for  $E_G=1.95$  eV. Total current density, electron and hole current densities through IB ( $J_{genIB,1}/X$  and  $J_{genIB,2}/X$ ) and the current density resulting from the transitions between VB to CB ( $J_{cv}/X$ ) have been analyzed. It was seen that the total current density at maximum power point was maximum, when  $J_{genIB,1}/X$  and  $J_{genIB,2}/X$  became equal. So the positions of IB level when  $J_{genIB,1}/X$  and  $J_{genIB,2}/X$  become equal are called as the optimum IB levels.  $J_{cv}/X$  has been found as independent of the position of IB level. In the case of  $\gamma=1$ , overlap caused the optimum IB level to shift towards the half of the bandgap and  $J_{cv}/X$  to decrease sharply. The variation of optimum IB level was negligible and the reduction in  $J_{cv}/X$  was minimized in  $\gamma=10$  case. As a result, this study has given complementary informations and comments about the effect of overlap on the efficiency of IBSC.

#### 5. References

- [1] A. Luque, Marti A., "Increasing the efficiency of ideal solar cells by photon induced transitions at intermediate levels", *Phys. Rev.Lett.*, vol. 78, no.26, pp. 5014–5017, Jun., 1997.
- [2] T. S. Navruz, M. Saritas, "Efficiency variation of the intermediate band solar cell due to the overlap between absorption coefficients", *Sol. Energy Mater. Sol. Cells*, vol. 92, no. 3, pp. 273-282, Mar., 2008.
- [3] T. S. Navruz, "Efficiency optimization of intermediate band solar cell", P.Hd. Thesis, Dept. of Electrical&Electronics Eng., Gazi Univ., My., 2008, Ankara.
- [4] T. S. Navruz, M. Saritas, "The effect of Auger mechanism on the efficiency of the intermediate band solar cell", *22nd European Photovoltaic Solar Energy Conference*, Milan, Italy, 2007, pp. 641-647.
- [5] M. Ley, J. Boudaden, Z.T. Kuznicki, "Thermodynamic efficiency of an intermediate band photovoltaic cell with low threshold Auger generation", *J. Appl. Phys.*, vol. 98, no. 4, pp. 44905 1-5, Aug., 2005.
- [6] A.S. Browna, M. A. Green, "Intermediate band solar cell with many bands: Ideal performance", *J. Appl. Phys.*, vol. 94, no. 9, pp. 6150- 6158, Nov., 2003.
- [7] A. Luque, A. Marti, "A metallic intermediate band high efficiency solar cell", *Prog. Photovolt*, vol. 9, no. 2, pp. 73–86, April, 2001.
- [8] A. Marti, L. Cuadra, A. Luque, "Quasi drift-diffusion model for the quantum dot intermediate band solar cell", *IEEE Trans. Electron Dev.*, vol. 49, no. 9, pp. 1632–1639, Sept, 2002.
- [9] N. Lopez, A. Marti, A. Luque, C. Stanley, C. Farmer, P. Diaz, "Experimental Analysis of the Operation of Quantum Dot Intermediate Band Solar Cells", *J. Sol. Energy Eng.*, vol.129, no. 3, pp. 319-322, Aug., 2007.